Effects of ring number and baffled-ring distances on ultrafiltration in the tubular membrane inserted concentrically with a ring rod

Ho-Ming Yeh*, Chii-Dong Ho and Cha-Hsin Li

Energy and Opto-Electronic Materials Research Center,Department of Chemical and Materials Engineering, Tamkang University, Tamsui, Taipei County251, Taiwan

(Received May 19, 2011, Revised December 26, 2011, Accepted January 06, 2011)

Abstract: The permeate flux declination along an ultrafilter membrane is due mainly to the concentration-polarization resistance increment and the decline in transmembrane pressure. It was found in previous works that the concentration polarization resistance could be reduced in a ring-rod tubular membrane ultrafilter using the turbulent behavior. In the present study, the performance was further improved by properly and gradually decreasing the baffled-ring distance along the cross-flow channel coupled with properly adjusting the number of baffled rings. This theoretical analysis is based on the mass and momentum balances as well as the application of the resistance-in-series model. The correlation predictions are confirmed with the experimental results for dextran T500 aqueous solution ultrafiltration.

Keywords: ultrafiltration; tubular membrane; ring-rod insert; baffled-ring distance; proper ring number

1. Introduction

In cross-flow ultrafiltration, the permeate flux generally declines along the flow channel due to the concentration polarization phenomenon by the rejected particles (Nokao *et al*. 1979, Clifton *et al*. 1984). Recently, several technical approaches developed for reducing the effects of concentration polarization and progressive fouling to enhance the permeate flux have been thoroughly discussed (Bhattacharjee and Bhattacharya 2006, Ghidossi *et al*. 2006, Barbot and Moulin 2008) The mechanisms of colloidal natural organic matter fouling in ultrafiltration (Costa *et al*. 2006), and the elucidation of fouling mechanisms and fouling control by membrane surface modification (Susanto *et al*. 2008) have been also investigated. It was reported that gradually increasing the turbulent strength along the flow channel might suitably suppress the increasing resistance to permeation due to concentration polarization while properly maintaining the decreasing transmembrane pressure (Fontes 2005). The improvements of ultrafiltration in the tubular membranes inserted concentrically with solid rod have been investigated either by varying rod radius (Yeh and Chen 2009), or by wrapping a wire on the solid rod with increasing wire incidental angles (Yeh and Chen 2006), as well as with various ring distances (Yeh 2010). The purpose of this study is to investigate the ultrafiltration permeate flux improvement in a tubular membrane by inserting a concentric ring rod with baffled ring distances varying along the membrane tube to gradually enhance the turbulent behavior and, thus, to reduce the ultrafiltration resistance due to concentration polarization. The baffled ring

* Corresponding author, Professor, E-mail: hmyeh@mail.tku.edu.tw

distances are gradually decreased along the flow channel with properly adjusting the number of rings. The effects of baffled-ring numbers and distances on permeation are discussed.

2. Analysis

Consider a tubular-membrane module of length L and radius r_m inserted concentrically with a solid rod of radius kr_m, wrapped with (N-1) baffle rings with gradually decreasing ring distances d_j along the solid rod in an arithmetic series of constant difference a, as shown in Fig. 1, i.e.,

$$L = \sum_{j=1}^{N} d_j = \sum_{j=1}^{N} [d_1 - (j-1)a], \quad j = 1,2,3,..., N \tag{1}$$

where N denotes the number of sections between two baffled rings.

2.1 Mass balance

Let Q(z) be the solution volume flow rate in a rind-rod membrane tube and J(z) be the permeate flux by ultrafiltraion. The mass balance over a slice dz of the flow channel is then

$$\frac{dQ}{dz} = -2\pi r_m J \tag{2}$$

Because the membrane ultrafiltration permeation is much smaller than the volume flow rate Q, J in Eq. (2) may be approximately taken as its average value for calculating the volum flow rate declination, i.e.,

$$\bar{J} = \frac{1}{L}\int_0^L J(z)dz \tag{3}$$

The volume flow rate declination behavior along the tube is readily obtained by integrating Eq. (2) with the entrance condition: $Q = Q_i$ at $z = 0$, as

$$Q = Q_i - 2\pi r_m \bar{J} z \tag{4}$$

and the volume flow rate at the outlet, z=L, is

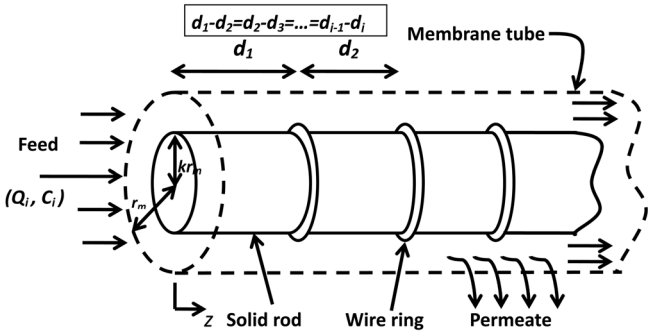

Fig. 1 An ultrafilter membrane inserted with a ring rod.

$$Q_0 = Q_i - 2\pi r_m \bar{J} L \tag{5}$$

where the bulk velocity distribution along the tube is related to the inlet velocity u_i as

$$u_b(z) = u_i - \frac{2\bar{J}z}{r_m(1-k^2)} \tag{6}$$

where

$$u_i = \frac{Q_i}{[\pi r_m^2(1-k^2)]} \tag{7}$$

2.2 Momentum balance

Taking momentum balance over a slice dz of the flow channel, one has

$$\rho\frac{du_b^2}{dz}[\pi r_m^2(1-k^2)] + \frac{d(\Delta P)}{dz}[\pi r_m^2(1-k^2)]dz + 2\pi r_m(\tau_1 + k\tau_2)dz = 0 \tag{8}$$

where $\Delta P = (P - P_S)$, denoting the transmembrane pressure, and $P(z)$ and P_s are the pressures in the tube and shell sides, respectively, while τ_1 and τ_2 are the shear stresses on the membrane and ring-rod surfaces, respectively. Since the shear stress τ_1 is related to the friction factor f_1 as

$$\tau_1 = \frac{f_1 \rho u_b^2}{2} \tag{9}$$

we have the momentum balance equations as

$$\rho\frac{du_b^2}{dz} + \frac{d(\Delta P)}{dz} + \frac{\bar{f}\ \rho u_b^2}{r_m(1-k^2)} = 0 \tag{10}$$

where $\bar{f}$ denotes the total average friction factor defined by

$$\bar{f} = f_1 + kf_2 \tag{11}$$

in which k is the rod radius to tube radius ratio.

2.3 Declination of transmembrane pressure

Integrating Eq. (10) from $z = 0$ ($\Delta P = \Delta P_i$) to $z = z$, one has the transmembrane pressure declination along the flow channel as

$$\Delta P = \Delta P_i - \rho(u_b^2 - u_i^2) - \frac{\bar{f}\rho}{r_m(1-k^2)}\int_0^z u_b^2 dz \tag{12}$$

Substitution of Eq. (6) into the above equation yields

$$\Delta P = \Delta P_i + [2\rho\bar{J}/\{r_m(1-k^2)\}][u_i\{2-(\bar{f}u_i/2\bar{J})\}z + \{2\bar{J}/r_m(1-k^2)\}\{(\bar{f}u_i/2\bar{J})-1\}z^2 + (\bar{f}/6\bar{J})\{2\bar{J}/r_m(1-k^2)\}^2 z^3] \tag{13}$$

2.4 Permeate flux

The resistance-in-series model may be employed to express the permeate flux as (Yeh and Chen 2006)

$$J(z) = \frac{\Delta P(z)}{R_m + R_f + \phi \Delta P(z)} \tag{14}$$

where R_m denotes the intrinsic membrane resistance, R_f is the resistance due to fouling phenomena, such as solute adsorption, while $\phi\Delta P(z)$ is the resistance due to the concentration polarization/gel layer, which will be proportional to the amount and specific hydraulic resistance of the compressible layer deposited and may be assumed to be a linear function of the transmembrane pressure with ϕ as a proportional constant. The values of R_m, R_f and ϕ value will be determined experimentally. The local permeate flux J(z) is readily calculated numerically by substituting Eqs. (6) and (12) into Eq. (13). The average permeate is estimated by Eq. (3) using the iteration method.

3. Experiment

3.1 Experimental conditions

The experimental apparatus (Fig. 2), materials and procedure were exactly the same as those in the previous work (Yeh 2010), except that the membrane tube with radius r_m of 3 mm and length L of 0.4 mm inserted with a solid rod of radius kr_m(k = 1/2), was wrapped with (N-1) ring wires of 1 mm diameter. Accordingly, there were N (=1, 5, 10, and 20) sections between the ring wires, as shown in Fig. 1. The distance between two rings d_j at the jth section decreases along the steel rod using an arithmetic series with constant difference a, as shown in Eq. (1). Eq. (1) may be rewriter as

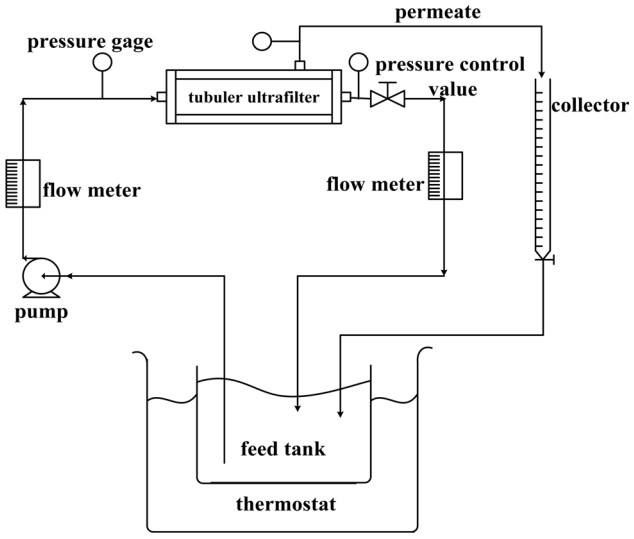

Fig. 2 The experimental apparatus of membrane ultrafiltration.

$$L = \sum_{j=1}^{N} d_j = Nd_1 - \frac{N(N-1)a}{2} \tag{15}$$

And thus

$$d_1 = (L/N) + \frac{(N-1)a}{2} \tag{16}$$

The tested solution was dextran T500 aqueous solution. The fouling mechanisms by dextran would be different from molecular weights, (MW) i.e., greater MW for cake layer formation, and small MW for concentration polarization. The feed solution concentrations C_i were 0.1, 0.2, 0.5 and 1.0 wt% dextran T500, the feed flow rates Q_i were 1.67, 2.50, 3.33 and 4.17 cm^3/s, and the inlet transmembrane pressure ΔP_i were 30, 50, 80, 115 and 140 kPa. The physical properties of feed solution are $\rho = 1000$ kg/m^3 and $\mu = 0.894\times10^{-3}e^{0.408Ci}$ (kg/m·s) (Yeh and Chen 2006). Many experimental results for average permeate flux $\bar{J}$ were obtained, as well as the outlet transmembrane pressure ΔP_0 and solution volumetric flow rate Q_0 were measured, under various operating conditions. Some of the results for $\bar{J}$ are plotted in Figs. 3-6 for $C_i = 0.1$ and 0.5 wt%.

3.2 Correlation equations for R_m, R_f and ϕ

The ϕ and $(R_m + R_f)$ values were determined graphically from the experimental data of $(\bar{J})_{exp}$ and $(\overline{\Delta P})_{exp} = [(\Delta P_i + \Delta P_0)/2]_{exp}$ for various operating conditions (C_i, ΔP_i and $u_i = Q_i/\pi r_m^2(1-k^2)$), by following the same procedures performed in previous works (Yeh 2010) with Eq. (13) modified, as

$$\frac{1}{(\bar{J})_{exp}} = \phi + \frac{R_m + R_f}{(\overline{\Delta P})_{exp}} \tag{17}$$

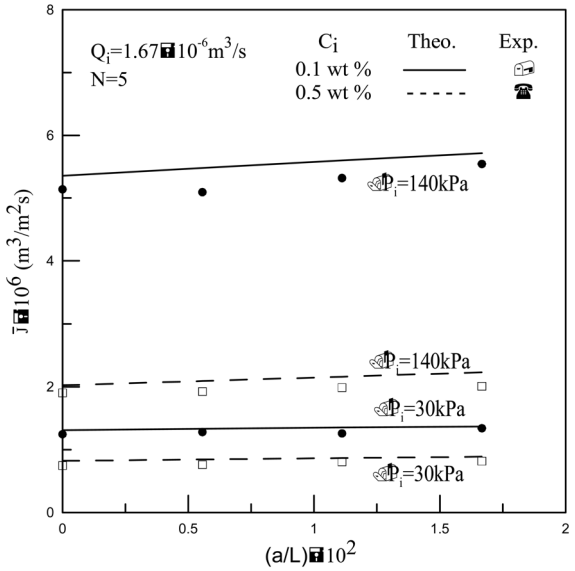

Fig. 3 $\bar{J}$ vs. (a/L) for $Q_i = 1.67\times10^{-6}$ m^3/s and N=5 with ΔP_i as parameter.

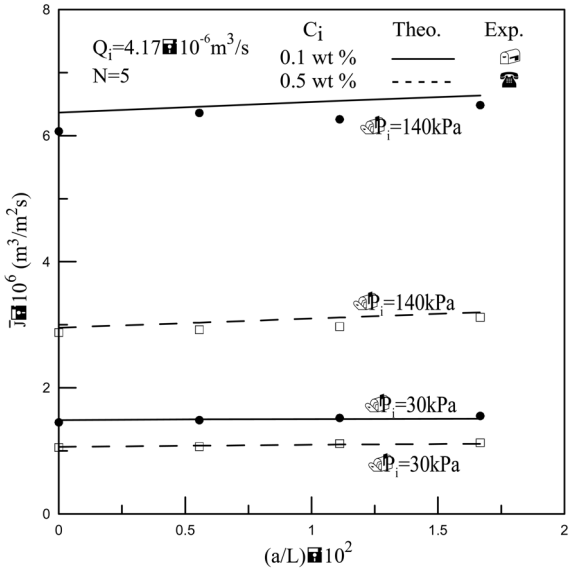

Fig. 4 $\bar{J}$ vs. (a/L) for $Q_i = 4.17\times10^{-6}$ m^3/s and N=5 with ΔP_i as parameter.

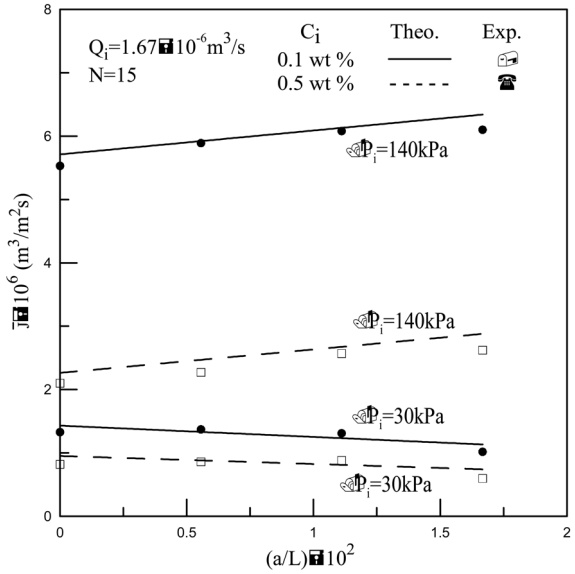

Fig. 5 $\bar{J}$ vs. (a/L) for $Q_i = 1.67\times10^{-6}$ m^3/s and N=15 with ΔP_i as parameter.

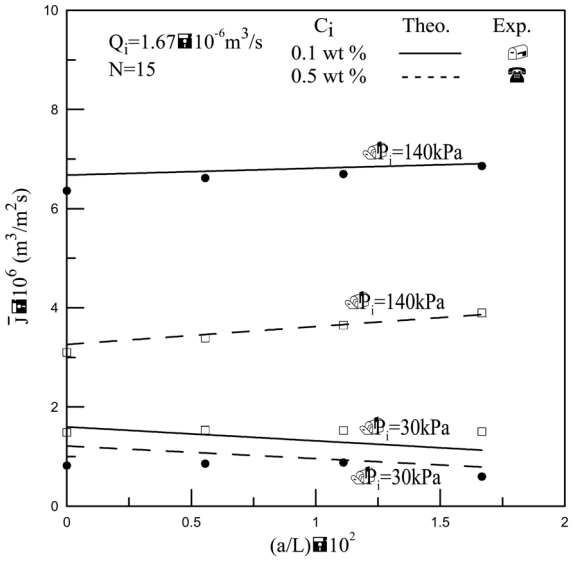

Fig. 6 $\bar{J}$ vs. (a/L) for $Q_i = 4.17\times10^{-6}$ m^3/s and N=15 with ΔP_i as parameter.

With the experimental data it was found that a plot of $1/(\bar{J})_{exp}$ vs. $1/(\overline{\Delta P})_{exp}$ at certain u_i and C_i could be constructed as a straight line using the least squares method. The values for the intersection of ordinate (ϕ) and the slope ($R_m + R_f$) were determined as function of u_i and C_i. The correlation equations for ϕ and ($R_m + R_f$) were constructed using the least squares method as a function of u_i, C_i, N and a/(L/N) with L=0.4 m and N=1, 5, 10, 15, 20, i.e., (Li 2007)

$$\phi = 2.711\times10^{5}u_i^{-0.565}C_i^{1.38}N^{-0.128}\left[1-\frac{a}{(L/N)}\right]^{1.082},\ \text{s/m} \tag{18}$$

$$R_m+R_f = 1.63\times10^{10}+4.305\times10^{9}u_i^{-0.644}C_i^{0.442}N^{-0.148}\left[1-\frac{a}{(L/N)}\right]^{3.423},\ \text{Pa·s/m} \tag{19}$$

3.3 Correlation equations for $\bar{f}$

The overall friction factor may be determined experimentally from Eq. (10) using Eq. (6) and the experimental values measured at the inlet (ΔP_i, Q_i) and at the outlet (ΔP_o, Q_o), i.e.,

$$\frac{\Delta P_i-(\Delta P_o)_{exp}}{L} = \frac{\bar{f}\rho[(Q_i+Q_0)_{exp}/2]^2}{\pi^2 r_m^5(1-k^2)^3}+\frac{\rho(Q_i^2-Q_o^2)_{exp}}{\pi^2 r_m^4(1-k^2)^2} \tag{20}$$

or

$$\bar{f} = \frac{\pi^2 r_m^5(1-k^2)^3[\Delta P_i-(\Delta P_o)_{exp}]}{L\rho[(Q_i+Q_0)_{exp}/2]^2}-4r_m(1-k^2)\left(\frac{Q_i-Q_0}{Q_i+Q_0}\right)_{exp} \tag{21}$$

and the volumetric flow rate at the outlet (z=L) is estimable from Eq. (5), as

$$(Q_0)_{exp} = Q_i - 2\pi r_m L(\bar{J})_{exp} \tag{22}$$

Many values for $\bar{f}$ were thus obtained using the experimental data. The correlation equation for $\bar{f}$ was also constructed using the least squares method as a function of the Reynolds number, Re, ring number N and the ring distance variation factor, [a/(L/N)], i.e., (Li 2007)

$$\bar{f} = 7.59 \times 10^3 Re^{-1.89} N^{0.3} \left[1 - \frac{a}{(L/N)}\right]^{-9.012} \tag{23}$$

where (L/N) denotes the average ring distance, and the Reynolds number is defined as

$$Re = \rho \bar{u} D_e/\mu = (\rho/\mu)[(Q_i + Q_0)/\{2r_m^2 \pi(1 - k^2)\}][2(1 - k)r_m] = \rho(Q_i + Q_0)/[\mu\pi r_m(1 + k)] \tag{24}$$

in which $D_e = 2(1 - k)r_m$, is the equivalent diameter of the concentric tube.

4. Results and discussion

4.1 Comparison of correlation predictions with experimental results

The average permeate flux $\bar{J}$ were calculated numerically by substituting Eqs. (13) and (14) into Eq. (3), using the iteration method coupled with using the correlation equations, Eqs. (18), (19) and (23). Some of the predicted values are compared with the experimental data, as shown in Figs. 3-6 for C_i=0.1 and 0.5 wt%. Since the tendencies of the comparison of the predicted values with the experimental data for C_i=0.2 and 1.0 wt% dextran T500, are almost the same as those for C_i=0.1 and 0.5 wt%, they may be no need to be presented by other four similar figures. Figs. 3-6 show that most of the correlation predictions for the permeate flux are rather higher than those obtained in the experimental results, especially for higher transmembrane pressure (ΔP = 140 kPa) and small ring number (N = 5), as shown in Figs. 3 and 5. This deviation may be due to the pseudo-precise assumption made in the resistance-in-series model, Eq. (14), for the concentration polarization resistance, $\phi\Delta P(z)$. Accordingly, along the flow direction, the theoretical prediction of $\phi\Delta P(z)$ decreases slightly while, actually, the experimental values of concentration polarization resistance obviously increase. The average permeate flux increases with the inlet volume flow rate Q_i and transmembrane pressure ΔP_i, but decreases when the inlet concentration C_i increases.

4.2 Effect of (a/L) on concentration-polarization resistance

At the inlet, the concentration polarization layer thickness is smaller and then increases along the flow channel. Therefore, a larger entrance ring-distance (d_1/L) for producing smaller turbulent strength around the inlet region of a ring-baffle device, is sufficient enough to reduce the lower concentration polarization resistance there. In the meantime, a smaller ring distance, as well as stronger turbulent behavior, around the outlet region is required for suppressing the higher concentration polarization resistance. In this study, we are concerned with a device that gradually increases the turbulent behavior along the flow channel by gradually decreasing the N ring-baffle distances d_i using an arithmetic series of constant difference a, as defined by Eq. (1). Therefore, the higher concentration polarization resistance in the near end of the flow channel will decrease more rapidly by increasing (a/L) to make (d_1/L) larger and (d_N/L) smaller, as indicated by Eqs. (1) and (15). However, for the case of

Table 1 Experimental results of concentration polarization resistance $\phi(\Delta\overline{P})\times10^{-12}(Pa\cdot s/m)$ for $C_i = 0.5$ *wt*% and $N = 10$

$Q_i\times10^6$ (m^3/s)	$\Delta P_i\times10^{-5}$ (Pa)	$d_1 = 0.05$ *m* $(a/L) = 0.556\times10^{-2}$	$d_1 = 0.06$ *m* $(a/L) = 1.11\times10^{-2}$	$d_1 = 0.07$ *m* $(a/L) = 1.667\times10^{-2}$
1.67	30	1.020	1.006	0.983
	140	4.761	4.694	4.585
4.17	30	0.349	0.289	0.286
	140	1.630	1.347	1.336

larger N and lower ΔP_i, the small driving force (ΔP_i) will further decrease when N and (a/L) increase, leading to a decrease in the averaged permeate flux, as shown in Figs. 5 and 6 for N=15 and $\Delta P_i = 30$ kPa, as well as Figs. 8 and 10 for $(a/L) = 1.667\times10^{-2}$ and $\Delta P_i = 30$ kPa. The average concentration polarization resistance value, $\phi\Delta\overline{P}$, decreases when the constant difference, a, increases, as indicated by Eq. (18) for ϕ, also shown in Table 1 for $\phi\Delta P$.

4.3 Effects of N and (a/L) on total ultrafiltration resistances

The turbulent behavior in the cross-flow ultrafiltration may be strengthened either by increasing the number of baffled-ring section N or by increasing the dimensionless difference constant (a/L), resulting in a decrease in the total ultrafiltration resistances $(R_m + R_f + \phi\overline{\Delta P})$. This fact can be verified by Eqs. (18) and (19), and the results are more obvious for higher feed concentrations C_i where the resistances are larger, or for lower inlet fluid velocity.

4.4 Effects of N and (a/L) on average permeate flux

The increase in turbulent strength by either increasing the number of baffled-ring section, or by gradually decreasing the baffle-ring distance, actually has two conflicting effects on the permeate flux. The first is the desirable effect of decreasing the resistance to permeation due to the reduction in concentration polarization. This is good for ultrafiltration. The second is the undesirable effect of increasing the pressure drop, as well as decreasing the transmembrane pressure due to the increase in friction loss. This is bad for ultrafiltration. It appears, therefore, that proper turbulent strength adjustment along the flow channel with specified operating conditions (C_i, Q_i and ΔP_i), might effectively suppress any undesirable resistance to permeation due to concentration polarization while still preserving an effective transmembrane pressure, thereby leading to improved permeate recovery.

As seen in Figs. 3-6 for higher transmembrane pressure (say $\Delta P_i = 140$ kPa), the average permeate flux $\overline{J}$ increases when the baffle-ring distance d_j gradually decreases more rapidly along the flow channel, as well as when the dimensionless difference in the arithmetic series, (a/L), increases. Moreover, $\overline{J}$ also increases as N increases. This is because that for high transmembrane-pressure operation, either by increasing (a/L) or increasing N, the decrease in the resistance to permeation can still compensate for the decrease in transmembrane pressure. On the other hand, for operation under lower transmembrane pressure (say $\Delta P_i = 30$ kPa), the desirable effect no longer compensates for the undesirable effect and the permeate flux $\overline{J}$ decreases when (a/L) or N is larger, especially for lower volume flow rate, as shown in Figs. 5 and 6. Accordingly, for specified operating conditions (C_i, Q_i, ΔP_i), there may

Table 2 Experimental results of permeate flux for k = 1/2, N =1 and a =0

$Q_i\times10^6$ (m^3/s)	ΔP_i (kPa)	C_i = 0.1 wt%		C_i = 0.5 wt%	
		ΔP_0 (kPa)	$\bar{J}\times10^6$ (m/s)	ΔP_0 (kPa)	$\bar{J}\times10^6$ (m/s)
1.67	30	29.89	1.0142	29.20	0.7633
	140	139.65	4.4643	139.02	1.7544
4.17	30	29.69	1.3441	29.49	0.9042
	140	139.84	5.8593	139.45	2.2531

exist optimal values for N and/or (a/L) for better permeate flux, especially when Q_i and ΔP_i are small.

4.5 Improvement in performance

The improvement in performance resulting from operating a tubular membrane inserted concentrically with a ring rod is best illustrated by calculating the percentage increase in permeate flux based on $\bar{J}_0$ obtained in a tubular membrane of same size inserted with a solid rod but without rings (k=1/2, N=1, and a=0)

$$I = \frac{\bar{J}-\bar{J}_0}{\bar{J}_0} \tag{25}$$

where some experimental results for $\bar{J}_o$ are listed in Table 2, and the results for I vs. N under various operating conditions are shown in Figs.7 and 10. These figures show that generally, the improvement in performance I increases either with the number of baffled rings N, or with the

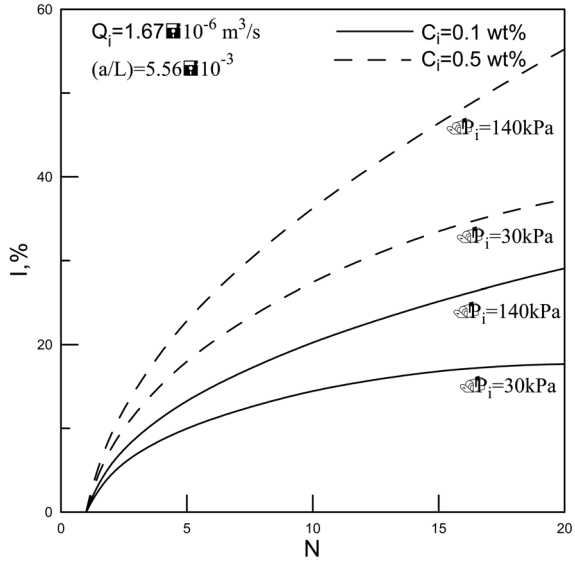

Fig. 7 I vs. N for $Q_i = 1.67\times10^{-6}$ m^3/s and $(a/L) = 5.56\times10^{-3}$ with ΔP_i as parameter.

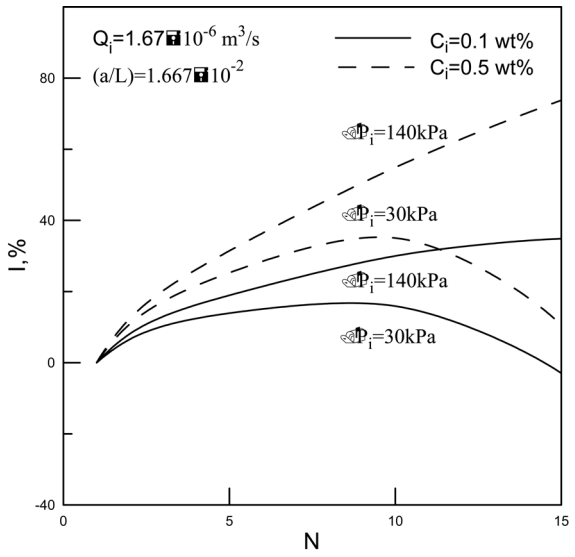

Fig. 8 I vs. N for $Q_i = 4.17\times10^{-6}$ m^3/s and $(a/L) = 1.667\times10^{-2}$ with ΔP_i as parameter.

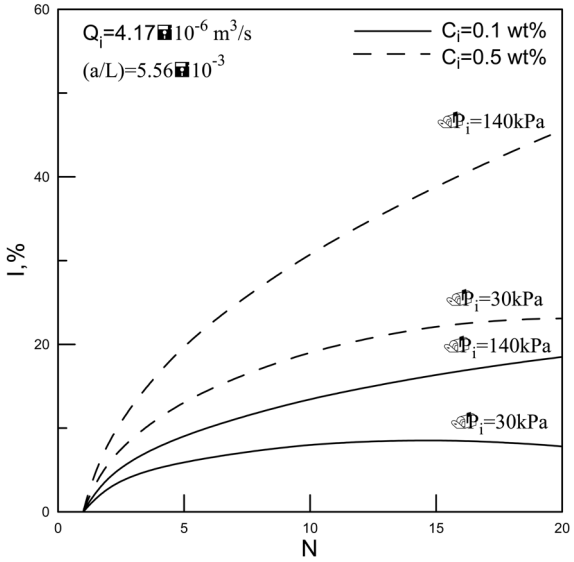

Fig. 9 I vs. N for $Q_i = 1.67\times10^{-6}\ m^3/s$ and $(a/L) = 5.56\times10^{-3}$ with ΔP_i as parameter.

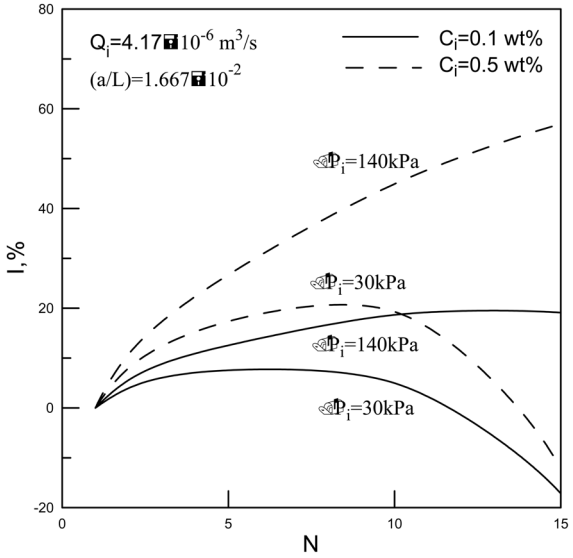

Fig. 10 I vs. N for $Q_i = 4.17\times10^{-6}\ m^3/s$ and $(a/L) = 1.667\times10^{-2}$ with ΔP_i as parameter.

dimensionless difference constant, (a/L). However, for operating with lower transmembrane pressure, $\Delta P = 30$ kPa, and larger (a/L), proper N and d_j (or a/L) exist for better performance. Consequently, considerable improvement in permeate flux is obtainable by employing a baffle-ring tubular membrane with the proper ring number N and proper ring distances d_j decreasing gradually along the ultrafilter, especially for higher feed concentration.

Fig. 10 shows that about 55% improvement is achieved when N=15 for $Q_i = 4.17\times10^{-6}$ m^3/s, $\Delta P_i = 140\ kPa$, $(a/L) = 1.667\times10^{-2}$, and $\Delta P_o = 135.01\ kPa$ (Li 2007). The energy consumption should be also taken into consideration for this critical operating condition and is estimated as follows

$$E = \rho Q_i \ell_{wf} = Q_i(\Delta P_i - \Delta P_o)$$
$$= (4.17\times10^{-6})(140 - 135.01)\times10^3 = 2.08\times10^{-2}\ \text{N·m/s}$$
$$= 2.79\times10^{-5}\ \text{hp} \tag{26}$$

Therefore, the increase in operating cost due to the increase in power consumption for baffled-ring rod inserted, may be ignored.

5. Conclusions

Ultrafiltration in a ring-rod tubular membrane with the proper ring number and properly decreasing baffled-ring distance along the tube membrane, was investigated both theoretically and experimentally. The ring-rod tubular membrane module was modified from a tubular membrane by inserting a steel rod concentrically wrapped with (N-1) baffled rings of gradually decreasing ring distance along the

module. Ultrafiltration of an aqueous dextrane T500 solution in the baffled-ring membrane tube of 0.4 m length (L), with the diameters of tube ($2r_m$= 6 mm), rod ($2kr_m$= 3 mm) and ring wire (1 mm), was carried out for various transmembrane pressures (ΔP_i), feed concentrations (C_i), feed flow rates (Q_i), ring number (N-1) and ring distances (d_j). The total number of baffled rings were fixed at 0, 4, 9, 14 and 19 (i.e., numbers of the sections between two baffled rings are N=1, 5, 10, 15 and 20) and their distances decreased gradually along the module, as indicated by Eq. (16). The present theoretical analysis is based on the mass and momentum balances coupled with resistance-in-series model application. The correlation predictions are scarcely higher than the experimental results.

Ultrafiltration in the module of same size inserted with a steal rod but without the baffled ring (k=1/2, N=1, a=0), was also carried out, and the results are presented in Table 2 for comparison with that obtained with baffled rings. In general, improvement in performance (I) increases when the number of ring N increases, or when the decrease in ring distance (a/L) is rather rapid, especially for higher feed concentrations, as shown in Figs. 7-10. This improvement is due to reduction in resistance to permeation. Actually, either increasing N or (a/L) will also decrease the transmembrane pressure. Nevertheless, the decrease in resistance to permeation can compensate for the decrease in transmembrane pressure for operating at higher transmembrane pressure. However, when operating at lower transmembrane pressure and larger dimensionless difference constant of an arithmetic series, there exists a proper N and (a/L) for better ultrafiltration, as shown in Figs. 3-10.

In usual, hollow fiber module is more preferable in terms of packing density of ultrafilter fibers than tubular module, and the weight of a tubular module will become heavier if a ring rod is inserted, leading to engineering problems. Nevertheless, in practical applications the size of ring-rod module may be reduced, say r_m=1 mm, k=1/2 and ring diameter=1/3 mm, and the materials of both rod and rings may be replaced with lighter materials, instead of steel.

References

Barbot, E. and Moulin, P. (2008), "Swimming pool water treatment by ultrafiltration-adsorption process", *J. Membr. Sci*., **314**(1-2), 50-57.

Bhattacharjee, C. and Bhattacharya, P.K. (2006), "Ultrafiltration of black liquid using disk membrane module", *Sep. Puri. Technol.*, **49**(3), 281-290.

Costa, A.R., de Pinho, M.N., and Elimelech, M. (2006), "Mechanisms of colloidal natural organic matter fouling in ultrafiltration", *J. Membrane Sci.*, **281**(1-2), 716-725.

Clifton, M.J., Abidine, N., Aptel, P. and Sanchez, V. (1984), "Growth of the polarization layer in ultrafiltration with hollow-fiber membranes", *J. Membrane Sci.*, **21**(3), 233-246.

Fontes, S.R. (2005), "Mass transfer in microfiltration with laminar and turbulent flow marcromolecular solutions", *J. Membrane Sci*., **249**, 207-211.

Ghidossi, R., Daurelle, J.V., Veyret, D., and Moulin, P. (2006), "Simplified CFD approach of a hollow fiber ultrafiltration syatem", *Chem. Eng. J*., **123**(3), 117-125.

Li, C.H. (2007), "Permeate flux analysis of ultrafiltration in various tubular membrane modules", M. S. thesis, *Tamkang University*, Tamsui, Taipei Country, Taiwan.

Nakao, S.I., Nomura, T., and Kimura, S. (1979), "Characteristics of macromolecular gel layer formed on ultrafiltration tubular membrane", *AIChE J*., **25**(4), 615-622.

Susanto, H., Arafat, H., Janssen, E.M.L., and Ulbricht, M. (2008), "Ultrafiltration of polysaccharide-protein mixtures: Elucidation of fouling mechanisms and fouling control by membrane surface modification", *Sep. Ruri. Technal*., **63**(3), 558-565.

Yeh, H.M. and Chen, Y.F. (2006), "Momentum balance analysis of permeate flux for ultrafiltration in tubular membranes with gradually increasing incidental angles of a wired-rod insert", *J. Membrane Sci*., **278**(2), 205-

211.
Yeh, H.M. and Chen, Y.F. (2009), "Ultrafiltration in a turbular membrane inserted concentrically with a solid rod of varying radius for improved performance", *Desalination*, **247**(1-3), 476-489.
Yeh, H.M. (2010), "Effect of gradully varying baffled-ring distance on ultrafiltration in tubular membranes inserted concentrically with a ring rod", *Desalination Water Treat*., **26**(1-3), 236-242.

CC

Nomenclature

a	constant difference of an arithmetical series (m)
C_i	concentration of feed solution (wt. % dextran T500)
D_e	equivalent diameter of flow cross section (m)
d_j	ring distance between (j-1)th and jth rings (m)
$\bar{f}$	average overall friction factor
$\bar{f}_1$, $\bar{f}_2$	average friction factor on membrane and ring rod surfaces, respectively
I	improvement in permeate flux
J	permeate flux of solution ($m^3/m^2 \cdot s$)
$\bar{J}$	average value of J ($m^3/m^2 \cdot s$)
$\bar{J}_0$	$\bar{J}$ obtained without a ring rod ($m^3/m^2 \cdot s$)
kr_m	radius of steel rod (m)
L	effective length of membrane tube (m)
ℓw_f	friction loss (N·m/kg)
N	number of sections between two baffled rings
P	pressure distribution on the tube side (Pa)
P_s	uniform permeate pressure on the shell side (Pa)
ΔP	transmembrane pressure, $p-p_s$ (Pa)
Q	volume flow rate in a tubular-membrane module (m^3/s)
r_m	inside radius of membrane tube (m)
R_e	Reynolds number
R_f	resistance due to solute adsorption and fouling (Pa·s/m)
R_m	intrinsic resistance of membrane (Pa·s/m)
u_b	bulk fluid velocity in the flow channel (m/s)
$\bar{u}$	average velocity through the flow channel, $(Q_i + Q_0)/[2\pi r_m^2 (1 - k^2)]$ (m/s)
z	axial coordinate, flow direction (m)

Greek letters

ϕ	proportion constant ($m^2 \cdot s/m$)
τ_1, τ_2	shear stresses on membrane and ring-rod surfaces, respectively (Pa)
ρ	fluid density (kg/m^3)
μ	fluid viscosity (kg/m^3)

Subscripts

i	at the inlet
0	at the outlet